JCTC Journal of Chemical Theory and Computation

Br···O Complexes as Probes of Factors Affecting Halogen Bonding: Interactions of Bromobenzenes and Bromopyrimidines with Acetone

Kevin E. Riley,*,[†,‡] Jane S. Murray,[§,||] Peter Politzer,[§,||] Monica C. Concha,[§] and Pavel Hobza[†]

Institute of Organic Chemistry and Biochemistry, Academy of Sciences of the Czech Republic, Center for Biomolecules and Complex Molecular Systems and Department of Physical Chemistry, Palacky University, 771 46 Olomouc, Czech Republic, Department of Chemistry, P.O. Box 23346, University of Puerto Rico, Rio Piedras, PR 00931, Department of Chemistry, University of New Orleans, New Orleans, Louisiana 70148, and Department of Chemistry, Cleveland State University, Cleveland, Ohio 44115

Abstract: Halogen bonding is a unique type of noncovalent binding phenomenon in which a halogen atom interacts attractively with an electronegative atom such as oxygen or nitrogen. These types of interactions have been the subject of many recent investigations because of their potential in the development of new materials and pharmaceutical compounds. Recently, it was observed that most halogen bonding interactions in biological contexts involve close contacts between a halogen bound to an aromatic ring and a carbonyl oxygen on a protein's backbone structure. In this work we investigate interactions of substituted bromobenzenes and bromopyrimidines with acetone to ascertain the effects of various substituents upon the strengths of these interactions. It was found that replacement of ring hydrogens in these systems has dramatic effects upon the interaction strengths of the resulting complexes, which have interaction energies between −1.80 and −7.11 kcal/mol. Examination of the electrostatic potentials of the substituted bromobenzene and bromopyrimidine monomers indicates that the addition of substituents has a large influence upon the most positive electrostatic potential on the surface of the interacting bromine and thus modulates these halogen bonding interactions. Results obtained using the symmetry-adapted perturbation theory (SAPT) interaction energy decomposition procedure also indicate that electrostatic interactions play the key role in these halogen bonding interactions. These results have important implications in drug design and crystal engineering. Halogen bonds have been a subject of great interest in these fields because of their unique noncovalent bonding characteristics.

Introduction

It is widely known that intermolecular and intramolecular noncovalent interactions are very important for the structures and stabilities of a broad range of molecular complexes and crystals. The hydrogen bond, the chief mode of interaction of which is through electrostatic and charge-transfer (delocalization) forces, has been the subject of many investigations and can be said to be the best characterized type of noncovalent interaction. The role of dispersion (and stacking) forces throughout many facets of chemistry has received an increasing amount of attention in the past decade or so. In recent years, halogen bonds, which share many properties with hydrogen bonds (although perhaps having a larger dispersive contribution), have been recognized as playing

---

* To whom correspondence should be addressed. E-mail: kev.e.riley@gmail.com.

[†] Academy of Sciences of the Czech Republic, Center for Biomolecules and Complex Molecular Systems and Department of Physical Chemistry, Palacky University, 771 46 Olomouc, Czech Republic.

[‡] University of Puerto Rico.

[§] University of New Orleans.

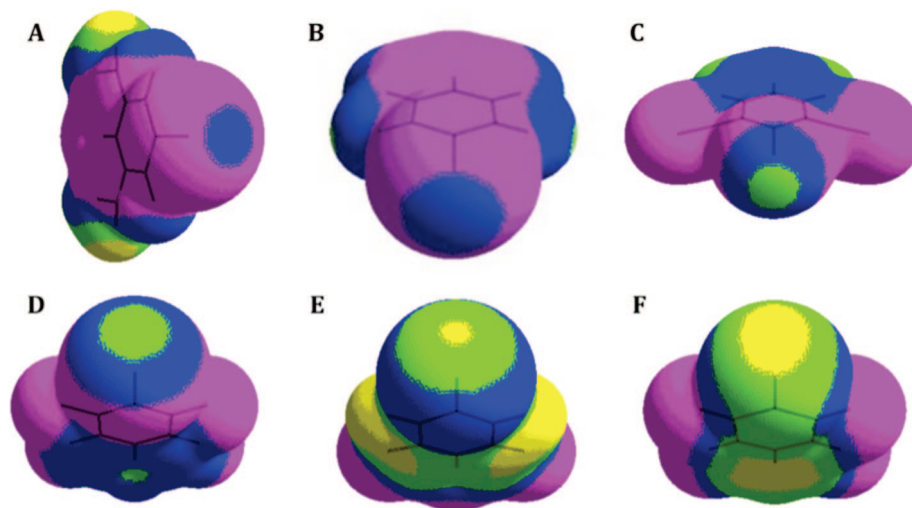[||] Cleveland State University.

Figure 1. Electrostatic potentials of selected bromobenzene molecules in order of increasing Br $V_{S,max}$: (A) 3,5-diaminobromobenzene, (B) bromobenzene, (C) 2,6-dicyanobromobenzene, (D) pentafluorobromobenzene, (E) *meta*-$C_6O_2H_3Br$ (**2**), (F) C_6O_4HBr (**3**). Color ranges, in kcal/mol, are purple, negative; blue, from 0 to 15; green, from 15 to 30; yellow, from 30 to 42. The bromine is facing the viewer in each plot.
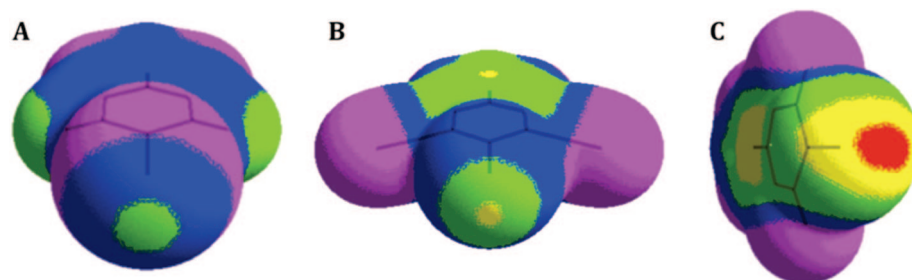

Figure 2. Electrostatic potentials of selected substituted bromopyrimidine molecules in order of increasing Br $V_{S,max}$: (A) 5-bromopyrimidne, (B) 5-bromo-4,6-dicyanopyrimidine, (C) $C_4N_2O_2HBr$ (**4**). Color ranges, in kcal/mol, are purple, negative; blue, from 0 to 15; green, from 15 to 30; yellow, from 30 to 42; red, greater than 42. The bromine is facing the viewer in each plot.

key roles in a wide variety of chemical systems. The phenomenon of halogen bonding has been a subject of particular interest within the fields of biochemistry [1,2] and materials science.[2,3] These types of interactions have recently been the subject of many theoretical [1,4−16] and experimental [17−19] investigations and promise to be of considerable significance in the development of novel chemical species with unique properties that may prove to be invaluable throughout chemistry and, more specifically, in drug design and crystal engineering. The importance of halogen bonds within various areas of scientific research is widely recognized, and this mode of interaction has been the subject of several recent review and perspectives articles.[3,4,20,21]

A halogen bond is a short-range RX···YZ interaction, where X is a halogen (typically chlorine, bromine, or iodine) that is part of the molecule RX and YZ is a Lewis base; Y is often an atom, such as oxygen, nitrogen, or sulfur, that has a lone pair.[3,4] Halogen bonds can be said to be analogous in many ways to hydrogen bonds (of the form RH···YZ) and are often treated in a similar manner. In both hydrogen bonding and halogen bonding, the donor (R) and the acceptor (Y) tend to be electronegative. For both hydrogen and halogen bonds, the distances H···Y and X···Y are generally less than the sum of the van der Waals radii of these atoms.

Because both halogen atoms and halogen bond acceptors (Y) are electronegative and are typically viewed as being negatively charged, the existence of halogen bonds is surprising and counterintuitive. However, studies of the electrostatic potentials of halogen-containing molecules by Brinck et al.,[5] Auffinger et al.,[1] and Politzer et al. [4,6] show that the larger halogens bound to carbon (and some other elements) often have a region of positive potential on the extension of the covalent bond to the halogen atom, that is, on the side of the halogen opposite to R (see the bromines in Figures 1B and 2A (bromobenzene and 5-bromopyrimidine)). The remainder of the halogen normally has also a negative region of potential, forming a ring around its lateral sides, except for cases where the molecule has one or more strongly electron-withdrawing groups.[6] The region of positive potential on a halogen's surface is often described as a positive σ-hole,[7] and has also been termed the electropositive crown.[1] The electrostatic attraction between the σ-hole and the negative Lewis base is the origin of halogen bonding. A halogen's σ-hole becomes larger and more positive as the size of the halogen increases, with a corresponding tendency for a halogen bond to become stronger.[4,6] Fluorine, the smallest (and most electronegative) halogen, rarely forms an electropositive crown, and thus does not normally

Br···O Complexes as Probes

J. Chem. Theory Comput., Vol. 5, No. 1, 2009 **157**

participate in halogen bonding. It has also been observed that the size and positive strength of the σ-hole tend to increase as R becomes more electron withdrawing.[4,6] Very recently, it has been demonstrated that covalently bonded atoms in Groups V and VI can also exhibit positive σ-holes and interact through these with Lewis bases.[8–10] It is interesting to note that the phenomenon of halogen bonding is attributable to a nonuniform atomic electron density and a corollary to this is that halogen bonds can only be properly treated using methods capable of accurately describing electron densities. Thus, molecular mechanics and molecular dynamics methods, which are based on parametrized force fields, would be expected to fail in describing halogen-bonding interactions.

The presence of a positive σ-hole on a halogen indicates that noncovalent interactions between that halogen and an electronegative atom should be highly electrostatic in nature. However, it should be kept in mind that halogen atoms, which are large and have large polarizabilities, would also be expected to interact with other chemical species through dispersion. In a recent work, the interactions between fluorinated and nonfluorinated halomethanes and formaldehyde (as well as methanol) were studied using high-level computational methods, including symmetry-adapted perturbation theory (SAPT).[11] It was found that these types of halogen-bonding interactions depend strongly upon electrostatic and dispersion contributions. The relative magnitudes of these are highly dependent upon the identity of the halogen X and the number of fluorine substituents in R, with the relative contribution of the electrostatic term increasing for larger X and higher degrees of fluorine substitution. These bonding tendencies correspond to the presence of larger and more positive σ-holes.

Halogen bonds involving oxygen as the acceptor Y are especially interesting in biochemistry because they are, by a large margin, the most common types of halogen bonds involved in protein−ligand interactions. Recently, Auffinger and co-workers carried out a crystallographic database survey of short halogen−oxygen distances[1] and found that 81 out of 113 X···O interactions involved carbonyl oxygens (the database contained 66 protein structures and 6 nucleic acid structures from the protein data bank). These interactions generally involved a protein's backbone carbonyl group (78 out of 81). Interactions involving hydroxyl oxygens were also fairly common (18 out of 113). In 73 of the 78 protein−ligand complexes that involve a carbonyl oxygen as the acceptor (∼94%), the halogen X is bonded to an aromatic or heterocyclic aromatic ring.

Clearly, halogen bonds in which R is aromatic (and heterocyclic aromatic) and Y is a carbonyl oxygen are among the most important in biological systems. In this work, we investigated the effects of various substituents on the electrostatic potentials (especially in the region of the halogen σ-holes), optimal complex geometries, and binding energies of bromobenzene−acetone and bromopyrimidine−acetone complexes. The substitution of various chemical groups on the aromatic rings in these complexes has a large effect on the halogen's interactive behavior and thus could be used in the design of novel (pharmaceutical) ligands. Here we
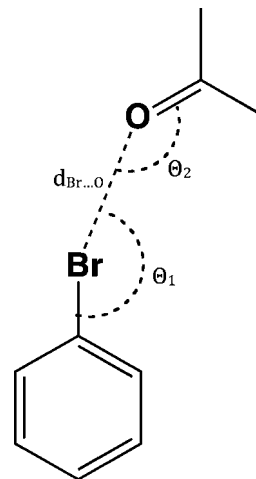

Figure 3. Schematic representation of $C_6H_5Br\cdots O=C(CH_3)_2$ halogen bond.

attempt to determine some of the fundamental rules for modifying a halogen bond's character via ring substitution.

Computational Methods

General. Halogen bonds are multifaceted types of interactions that depend strongly upon both electrostatic and dispersion forces. We have used several techniques to describe the halogen bonds occurring between variously substituted bromobenzenes and bromopyrimidines as donors and acetone as the acceptor. To study the geometrical and energetic parameters that govern these halogen bonds, we have obtained optimized intermolecular geometries and binding energies with the MP2 method and a mixed basis set, which describes bromine using the pseudo-potential-based aug-cc-pVDZ-PP and all other atoms with aug-cc-pVDZ. This approach is adopted because aug-cc-pVDZ-PP implicitly accounts for relativistic effects, which may influence halogen bonding interactions with such a large atom. We have computed the electrostatic potentials of all of the substituted bromobenzenes and bromopyrimidines, as well as that of acetone, at the B3PW91/6−31G(d,p) level. Finally, symmetry-adapted perturbation theory (SAPT) computations were performed to assess the relative contributions of dispersion and electrostatic (as well as induction and exchange) forces to the overall halogen bonding interactions. SAPT computations were performed using the aug-cc-pVDZ basis set.

Complete optimization of each of the halogen-bonding complexes described here proved to be too time-consuming and computationally costly to be practical. As a way to decrease the cost of these calculations, we divided the optimizations into two parts, first the monomers individually and then the dimer geometries in a self-consistent manner, using the optimal monomer geometries. The former were determined using the B3LYP/6-31G* method. To obtain optimal dimer geometries, the relative orientations of the monomers were systematically varied until the MP2/aug-cc-pVDZ(aug-cc-pVDZ-PP) binding energies reached self-consistency, as follows (see Figure 3 for geometric parameters):

1. The $d_{Br\cdots O}$ distance is changed by increments of 0.05 Å.

2. The angle θ_2 is varied by increments of one degree. θ_1 was assumed to be 180° for all complexes considered. The

validity of this assumption has been explored, and the results are described in the Results section. It should be noted that we have carried out a complete optimization for the case of the (unsubstituted) benzene-acetone complex at the MP2/ aug-cc-pVDZ level of theory (CP corrected, no pseudopotential), the resulting geometrical parameters for this optimized complex are $d_{Br\cdots O} = 3.13$ Å, $\theta_2 = 120.6°$, and $\theta_1 = 179.3°$; the geometrical values obtained using our "by-hand" method are $d_{Br\cdots O} = 3.15$ Å, $\theta_2 = 120°$, and $\theta_1 = 180°$ (by definition). We believe that the optimization procedure used here is sufficient to obtain final geometries that are very close to the potential energy minima for these complexes and that, given the present purpose of comparing halogen bonds with various aromatic substituents, the results obtained using this method will describe the important trends in terms of the effects of substituents on geometrical parameters. We will also note here that we carried out another optimization for the benzene−acetone complex using the DFT/B3LYP/ 6−31+G* method to determine whether or not a lower level method, which does not describe dispersion interaction contributions very well, could systematically be used for the purposes of geometry optimization in this study. It was found that the final geometry parameters obtained at this level of theory are as follows: $d_{Br\cdots O} = 3.30$Å, $\theta_2 = 130.7°$, and $\theta_1 = 178.9°$. These results are rather far from those obtained at the MP2/aug-cc-pVDZ level, with a $\Delta\theta_2$ of about 10° and $\Delta d_{Br\cdots O}$ of 0.13 Å. With this result in mind, we determined that the optimization of these complexes using DFT methods would not be appropriate for this study.

Interaction energies were calculated at the MP2/aug-cc-pVDZ/aug-cc-pVDZ-PP level of theory, which has been shown to give results that are at least semiquantitative for halogen bonds,[11] although there is a tendency to underestimate the strengths of the interactions. This is more pronounced for weak halogen bonds (which are generally more dispersive in nature) and becomes less important for strong ones (which are generally more electrostatic). ΔE is given by

$$\Delta E = E_{complex} - (E_{acetone} + E_{brominederivative}) \quad (1)$$

Here the counterpoise method was used to account for the basis set superposition error (for binding energies and optimization computations).[22]

In this work, our halogen bond donors are bromobenzene and bromopyrimidine derivatives and are listed in Tables 1 and 2. We have included a variety of functional groups (NH$_2$, OH, F, Cl, CN, and =O) in different combinations. It should be noted that among these are some carbonyl derivatives that may be unrealistic and might not exist for any extended period of time in nature (Table 2). The purpose of these unlikely structures, identified in Table 2 as **1**, **2**, **3**, and **4**, was to investigate the halogen bonding behavior of extreme examples of the bromobenzene and bromopyrimidine frameworks.
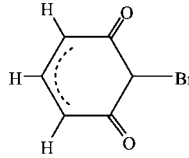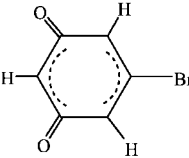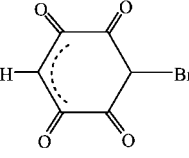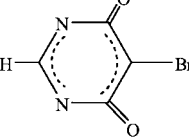
To compare the strengths of hydrogen bonds for complexes that are structurally similar to some of the halogen bonding complexes studied here, we have computed geometries and binding energies for the benzene−acetone and pentafluorobenzene−acetone complexes using the MP2/aug-cc-pVDZ

Table 1. Computed Bromine $V_{S,max}$ Values for a Series of Brominated Benzenes and Pyrimidines, and Interaction Energies, Optimized Br⋯O Separations, and Angles θ_2, for Their Complexes with Acetone[a]

molecule	Br $V_{S,max}$	interaction energy	Br⋯O separation	Br⋯O=C angle θ_2
bromobenzenes				
3,5-diaminobromobenzene	4.9	−1.80	3.15	120
para-aminobromobenzene	5.8	−2.02	3.10	121
meta-aminobromobenzene	7.1	−2.08	3.15	120
bromobenzene	9.7	−2.23	3.15	120
ortho-aminobromobenzene	9.9	−2.55	3.10	121
3,5-dihydroxybromobenzene	11.5	−2.25	3.10	121
ortho-chlorobromobenzene	12.9	−2.50	3.10	121
para-chlorobromobenzene	13.8	−2.52	3.10	121
meta-chlorobromobenzene	13.9	−2.53	3.10	121
3,5-difluorobromobenzene	15.7	−2.93	3.00	125
2,6-dicyanobromobenzene	22.1	−4.39	2.95	123
pentafluorobromobenzene	23.4	−4.08	2.95	124
3,5-dicyanobromobenzene	25.4	−3.71	2.95	127
bromopyrimidines				
2-bromopyrimidine	10.0	−2.46	3.05	121
5-bromopyrimidine	19.2	−3.24	3.00	125
5-bromo-4,6-dicyanopyrimidine	31.4	−5.04	2.75	125

[a] The $V_{S,max}$ and the interaction energies are in kcal/mol, Br⋯O separations in angstroms, and angles θ_2 in degrees.

Table 2. Computed Bromine $V_{S,max}$ Values for Four Brominated Carbonyl-Containing Heterocycles, and Interaction Energies, Optimized Br⋯O Separations, and Angles θ_1 and θ_2, for Their Complexes with Acetone[a]

Molecule	Br $V_{S,max}$	Interaction energy	Br⋯O separation	Br⋯O=C angle θ_2
1	15.1	−2.63	3.00	119
2	31.7	−4.30	2.95	129
3	38.5	−4.56	2.95	123
4	45.6	−7.11	2.80	129

[a] The $V_{S,max}$ and the interaction energies are in kcal/mol, Br⋯O separations in angstroms, and angles θ_2 in degrees.

method. The results obtained for these complexes can be directly compared with those for the bromobenzene-acetone and pentafluorobromobenzene-acetone complexes.

Br···O Complexes as Probes

J. Chem. Theory Comput., Vol. 5, No. 1, 2009 **159**

Electrostatic Potential $V(\mathbf{r})$. The electrostatic potential $V(\mathbf{r})$ that the electrons and nuclei of a molecule create at any point $\mathbf{r}$ in the surrounding space is given by eq 2.

$$V(\mathbf{r}) = \sum_A \frac{Z_A}{|\mathbf{R}_A - \mathbf{r}|} - \int \frac{\rho(\mathbf{r}')d\mathbf{r}'}{|\mathbf{r}' - \mathbf{r}|} \quad (2)$$

Z is the charge on nucleus A, located at $\mathbf{R}_A$, and $\rho(\mathbf{r})$ is the electronic density function of the molecule. $V(\mathbf{r})$ is positive in those regions in which the dominant contribution is that of the nuclei, negative where it is that of the electrons. The electrostatic potential is a physical observable, which can be determined experimentally by diffraction techniques[23,24] as well as computationally.

When using $V(\mathbf{r})$ to analyze noncovalent interactions, we normally compute it on the surface of the molecule, which we take, following Bader et al.,[24] to be the 0.001 au (electrons/bohr^3) contour of the molecule's electronic density. A surface defined as a three-dimensional contour of $\rho(\mathbf{r})$ has the advantage that it reflects features specific to that molecule, for example, lone pairs, π electrons, strained bonds, etc.

In a series of studies, it has been demonstrated that a variety of condensed phase physical properties that depend upon noncovalent interactions can be expressed quantitatively in terms of the features characterizing $V(\mathbf{r})$ on a molecular surface, which we label $V_S(\mathbf{r})$.[26,27] For example, empirical measures of hydrogen bond donating and accepting tendencies correlate well with the most positive values ($V_{S,max}$) associated with hydrogens and the most negative ($V_{S,min}$) on basic sites.[28]

SAPT Methodology. The SAPT method[31] permits the separation of interaction energies into physically meaningful components, such as those arising from dispersion, electrostatics, induction, and exchange. The SAPT interaction energy is given by eq 3.

$$E_{int} = E_{pol}^1 + E_{ex}^1 + E_{ind}^2 + E_{ex-ind}^2 + E_{disp}^2 + E_{ex-disp}^2 \quad (3)$$

Some of these terms can be combined to give commonly understood physical quantities. In this work, we define the following:

$E(\text{elec}) = E_{pol}^1$
$E(\text{ind}) = E_{ind}^2 + E_{ex-ind}^2$
$E(\text{disp}) = E_{disp}^2 + E_{ex-disp}^2$
$E(\text{exch}) = E_{ex}^1$ These four quantities refer to, respectively, the electrostatic, induction, dispersion and exchange contributions to the overall interaction energy.

In this work, we have utilized the SAPT technique to study the relative contributions of the various interaction energy terms in halogen-bonding systems. The systems studied here are relatively large, thus the only reasonable basis set that could be used for these computations is the aug-cc-pVDZ basis of Dunning. It should be noted that when SAPT is used with this medium -sized basis set, contributions from dispersion will generally be underestimated by approximately 10%−15%. The version of the SAPT method employed in this study utilizes electronic densities determined at the Hartree−Fock level.

All interaction energies and SAPT computations were carried out using the Molpro electronic structure package (M06).[30]

Results

Tables 1 and 2 give (a) the computed bromine $V_{S,max}$ values for a series of individual brominated benzene and pyrimidine derivatives, (b) their interaction energies with acetone, (c) the optimum Br···O separations, and (d) the angles θ_1 and θ_2. Here it can be seen that, as stated in the Introduction, the substitution of various groups onto the bromobenzene and bromopyrimidine rings has a very large effect upon halogen bond strengths. Computed interaction energies range from −1.80 (3,5-diaminobromobenzene) to −7.11 kcal/mol ($C_4N_2O_2HBr$, **4**). There are several other important aspects of these data that can immediately be seen in these tables. One of the most pronounced patterns is the relationship between interaction energies and Br $V_{S,max}$ values: Higher $V_{S,max}$ (more positive σ-holes) result in complexes that are more strongly bound. Also apparent is that the presence of electron-withdrawing groups on the aromatic rings results in higher bromine $V_{S,max}$ values and more negative interaction energies, while the electron-donating NH_2 substituent leads to weaker interactions. In terms of geometries, there are two prevailing trends: the bromine−oxygen separation ($d_{Br\cdots O}$) contracts and the angle θ_2 become larger as the interaction energy increases in magnitude (the latter of these two relationships shows only moderate correlation). Note that the Br···O separations, $d_{Br\cdots O}$, are all less than the sum of the bromine and oxygen van der Waals radii, 3.37 Å,[29] consistent with the occurrence of a noncovalent interaction.

Relation of Electrostatic Potentials to Interaction Energies. Figures 1 and 2 show the electrostatic potentials on the molecular surfaces of nine of the molecules listed in Tables 1 and 2. In each case, the $V_{S,max}$ on the bromine is along the extension of its C−Br bond. The bromine $V_{S,max}$ tends to increase relative to the parent molecule bromobenzene as electron-attracting components are introduced; these may be substituents (Figure 1) or ring nitrogens (Figure 2).

Figure 1 displays, in order of increasing $V_{S,max}$, the electrostatic potentials on the molecular surfaces of six of the bromobenzene derivatives. 3,5-diaminobromobenzene, Figure 1A, has the weakest $V_{S,max}$ in Tables 1 and 2, consistent with the electron-donating nature of the amino group. Moving on to electron-withdrawing substituents, we see that the five fluorines in pentafluorobromobenzene, Figure 1D, make the σ-hole more positive ($V_{S,max} = 23.4$ kcal/mol) than do the two ortho cyano groups in 2,6-dicyanobromobenzene ($V_{S,max} = 22.1$ kcal/mol), shown in Figure 1C. In the bromopyrimidine framework, however, in which the electron-attracting power of the cyano groups is complemented by that of two ring nitrogens, putting two ortho cyano groups on 5-bromopyrimidine framework, Figure 2B, increases the bromine $V_{S,max}$ to 31.4 kcal/mol. Finally, the introduction of carbonyl oxygens further strengthens the bromine σ-holes; C_6O_4HBr (**2**) and $C_4N_2O_2HBr$ (**4**), in Figures 1E and 2C, have $V_{S,max}$ of 38.5 and 45.6 kcal/mol, respectively. The latter is the most-positive bromine $V_{S,max}$ computed in this work.

The bromines in Figures 1A−D and 2A are more typical than are the others in Figures 1 and 2 in that they have rings of negative electrostatic potential around their lateral sides, while the surfaces of the bromines in Figures 1E and F and 2B and C are completely positive. These latter potentials are a consequence of the strongly electron-withdrawing substituents on the rings and have been noted earlier for bromine and other halogens in such environments.[6] For the molecules in Tables 1 and 2, we find that the more characterstic rings of negative electrostatic potential are no longer present after the bromine $V_{S,max}$ reaches about 30 kcal/mol.

As mentioned earlier, the data in Tables 1 and 2 show a general tendency for the interaction energies to increase in magnitude as the computed $V_{S,max}$ prior to interaction become more positive. There are some exceptions, primarily involving those molecules having ortho substituents. In such cases, there are often secondary interactions (favorable or unfavorable) between the acetone and the ortho groups that affect the interaction energies.[32] For a striking example, consider 3,5-dicyanobromobenzene and 2,6-dicyanobromobenzene (Table 1). 3,5-dicyanobromobenzene, which has its cyano groups meta to the bromine, has a $V_{S,max}$ of 25.4 kcal/mol. The interaction energy with acetone is −3.7 kcal/mol. Its ortho isomer, 2,6-dicyanobromobenzene, has a slightly weaker $V_{S,max}$ of 22.1 kcal/mol, yet a stronger interaction energy with acetone, −4.4 kcal/mol. This can be explained by looking at the surface electrostatic potential of 2,6-dicyanobromobenzene in Figure 1C. The negative potentials of the cyano nitrogens overlap with that on the lateral sides of the bromine, creating extended negative regions that can interact favorably with one or more acetone hydrogens. This complements the C=O···Br interaction, resulting in a more negative ΔE than for the 3,5-dicyano case.

An ortho substituent may also affect the bromine $V_{S,max}$ and hence ΔE through an overlapping of potentials. Thus the slightly lower bromine $V_{S,max}$ in *ortho*-chlorobromobenzene compared to the meta and para isomers may be caused by the chlorine's negative potential overlapping with the positive one of the bromine σ-hole.

Figure 4 shows a plot of interaction energy versus bromine $V_{S,max}$ for the 13 molecules lacking bulky ortho substituents. The correlation is remarkably good, with a correlation coefficient of 0.976. This demonstrates the importance of the positive σ-hole, as reflected by the computed bromine $V_{S,max}$, in determining the energetics of the C−Br···O halogen bonds. When all 20 molecules are included, the correlation coefficient drops slightly to 0.956. These correlations indicate the role that electrostatics plays in these interactions, whether or not there are secondary ones.

Relation of Binding Energies to Geometric Parameters. Figures 5−7 show the potential energy curves for five of the complexes, with respect to three geometrical parameters: the bromine−oxygen separation ($d_{Br···O}$), the Br···O−C angle (θ_2), and the C−Br···O angle (θ_1). These complexes are those of acetone with 3,5-diaminobromobenzene, bromobenzene, pentafluorobromobenzene, *meta*-C$_6$O$_2$H$_3$Br (**2**), and C$_4$N$_2$O$_2$HBr (**4**). These complexes are examples of halogen bonding interactions ranging from very weak (3,5-
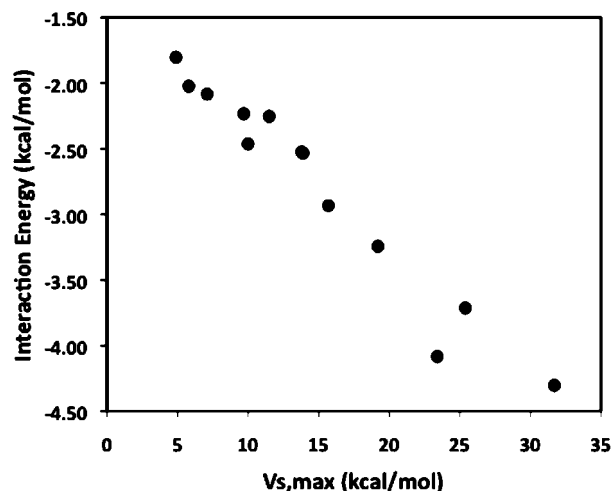

Figure 4. Plot of interaction energy vs bromine $V_{S,max}$ for the 13 molecules without ortho substituents (other than F). $R =$ 0.976.
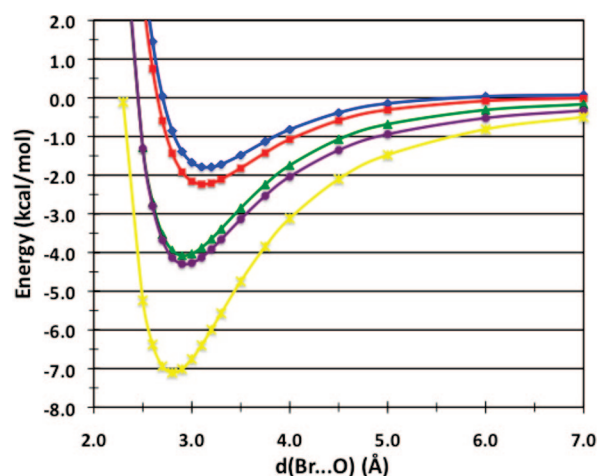

Figure 5. Potential energy curves for interaction energies with acetone as a function of the Br···O separation for complexes of 3,5-diaminobromobenzene (blue), bromobenzene (red), pentafluorobenzene (green), *meta*-C$_6$O$_2$H$_3$Br, **2** (purple), and C$_4$N$_2$O$_2$HBr, **4** (yellow).

diaminobromobenzene, $\Delta E = \mu 1.80$ kcal/mol) to very strong (**4**, $\Delta E = \mu 7.11$ kcal/mol). The general tendency for stronger halogen bonds to have shorter optimum Br···O separations can clearly be seen in Figure 5. It is also interesting to note that these halogen bonding interactions act over a relatively large distance, with the stronger ones still discernible at a radial distance of 7.0 Å.

The curves given in Figure 6 show that the interaction energy behaves is a shallow function of the Br···O−C angle (θ_2) between the values of approximately 115° and 180°. For these complexes, the difference between the interaction energies at the optimum angle and at 180° ranges from −0.32 (**2**) to −0.81 kcal/mol (3,5-diaminobromobenzene). As indicated in Tables 1 and 2, there is some tendency for the optimum Br···O−C angles to be larger for complexes with stronger interaction energies than for more weakly bound ones. These phenomena can be explained by looking at the electrostatic potential on the molecular surface of acetone, shown in Figure 8. The most striking feature is the strong
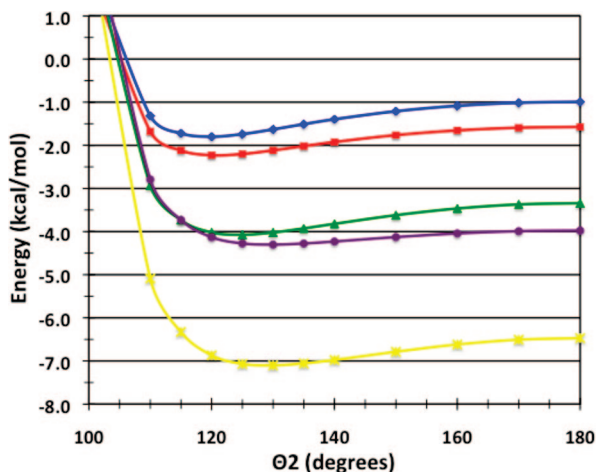
Br···O Complexes as Probes

J. Chem. Theory Comput., Vol. 5, No. 1, 2009 **161**

Figure 6. Potential energy curves for interaction energies with acetone as a function of the Br···O=C angle angle θ_2 for complexes of 3,5-diaminobromobenzene (blue), bromobenzene (red), pentafluorobenzene (green), *meta*-$C_6O_2H_3Br$, **2** (purple), and $C_4N_2O_2HBr$, **4** (yellow).

Figure 7. Potential energy curves for interaction energies with acetone as a function of the C−Br···O angle angle θ_1 for complexes of 3,5-diaminobromobenzene (blue), bromobenzene (red), pentafluorobenzene (green), *meta*-$C_6O_2H_3Br$, **2** (purple), and $C_4N_2O_2HBr$, **4** (yellow).
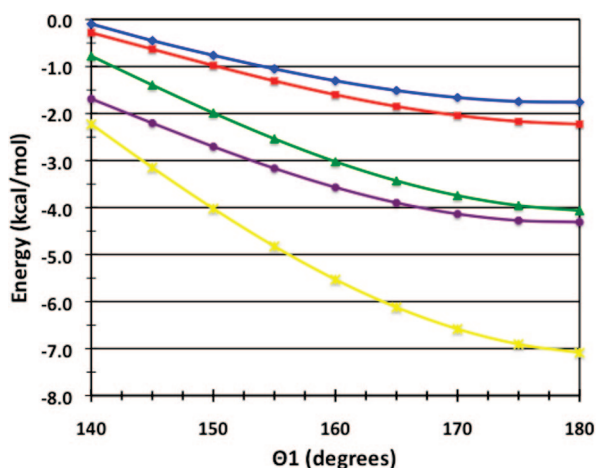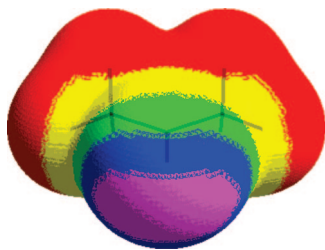

Figure 8. Electrostatic potential of acetone. Color ranges, in kcal/mol, are purple, more negative than −35; blue, from −35 to −30; green, from −30 to −20; yellow, from −20 to 0; red, greater than 0. The oxygen is toward the viewer.

band of negative potential, shown in purple, along the outer portion of the oxygen, extending 60° to either side of the C=O bond. This region has two minima, $V_{S,min}$, with values of −36.6 kcal/mol; however they are very shallow minima. This explains the fact that, although our calculations find the preferred C=O···Br angles for complexes with acetone

to be between 119° and 129°, the binding energies remain fairly strong as these angles increase from their optimum values to 180°. The slight trend of the optimum binding angle for more strongly interacting complexes to be larger may be attributable to the fact that stronger halogen bonding interactions are generally more electrostatic in nature and thus the bromine σ-hole has a greater tendency to align with the most negative regions in the space surrounding the carbonyl oxygen. These carbonyl oxygen global minima (V_{min}) are at angles (C−O−V_{min}) of ~127°.

A final observation that can be made from the data in Figure 6 is that the potential energy curve for the **2**···acetone complex is significantly shallower (although much more negative) than that of the pentafluorobromobenzene complex. The electrostatic potentials for these two molecules (Figure 1D and E) show that **2** does not have a typical σ-hole, with a ring of negative potential around the bromine. The fact that the entire bromine is positive in **2** allows it to interact attractively with the acetone oxygen over a wider range of angles.

Figure 7 shows binding energies as functions of the C−Br···O angle (θ_1). For all of the complexes, the optimum value of θ_1 is 180°, which corresponds to the optimal alignment of the bromine σ-hole with the carbonyl oxygen. The strengths of the interactions decrease rather sharply as θ_1 contracts, with ΔE for the weaker interactions (3,5-diaminobromobenzene and bromobenzene) reaching negligible values at 140°. This trend can clearly be attributed to the fact that the bromine σ-holes are no longer oriented toward the carbonyl negative charge density at low θ_1. As might be expected, the interaction energy falls off more slowly for the **2**···acetone complex than for that of pentafluorobromobenzene. This is the result of the overall positive potential found on the bromine atom of **2**, which can have an attractive electrostatic interaction over a wider range of the θ_1.

On the other hand, the strength of the **4**···acetone complex is highly dependent upon the strong electrostatic interaction with the more localized positive σ-hole of the bromine ($V_{S,max}$ = 45.6 kcal/mol). Figure 2C shows that the region of maximum positive potential on the bromine of **4** is relatively small. This explains the relatively sharp falloff for the interaction energy of this complex as a function of θ_1.

Comparison of Halogen Bonding and Hydrogen Bonding. It is interesting to compare the properties of halogen bonds with their, more ubiquitous, counterparts, hydrogen bonds. These types of intermolecular interactions evidently share several characteristics, most notably, both are interactions that occur between two atoms, which distinguishes them from general dispersion interactions and stacking interactions, which generally involve several atoms on both monomers. Another characteristic shared by both these types of noncovalent interactions is a large contribution of electrostatic forces to the overall interaction, although it should be noted that the electrostatic contribution to hydrogen bonding interactions is generally greater than that for most halogen bonding interactions.

Table 3 shows the interaction energies, $d_{X···O}$ distances, and X···O−C (θ_2) angles for the complexes of bromoben-

Table 3. Comparison of Halogen-Bonding and Hydrogen-Bonding Geometrical Parameters and Binding Energies[a]

molecule	interaction energy	X···O separation	X···O=C angle θ_2
halogen bond			
bromobenzene	−2.23	3.15	120
pentafluorobromobenzene	−4.08	2.95	124
hydrogen bond			
benzene	−2.01	2.50	113
pentafluorobenzene	−3.99	2.25	130

[a] The interaction energies are in kcal/mol, Br···O separations in angstroms, and angles θ_2 in degrees.

Table 4. Computed Symmetry-Adapted Perturbation Theory (SAPT) Interaction Energy Decomposition Values for Halogen-Bonding Complexes[a]

SAPT term	$C_6H_5Br···O=C(CH_3)_2$	$HC_4N_2O_2Br···O=C(CH_3)_2$
E(elec.)	−2.44	−10.10
E(ind.)	−0.61	−1.90
E(disp.)	−2.56	−3.67
E(exch.)	3.69	8.28
E(SAPT)	−1.92	−7.39

[a] In kcal/mol.

zene, pentafluorobromobenzene, benzene, and pentafluorobenzene with acetone. Here it can be seen that, for both cases, the halogen-bonding interactions are predicted to be slightly stronger than the hydrogen-bonding interactions; in the unsubstituted case (bromobenzene and benzene), the halogen bonding interaction energy is about 0.2 kcal/mol lower than that for the hydrogen bonding case, while the difference is about 0.1 kcal/mol for the fluorine substituted complexes. As would be expected, the $d_{X···O}$ distances are substantially shorter for the hydrogen-bonding complexes (by 0.65−0.70 Å). Interestingly, the X···O−C angle is larger for the bromobenzene complex than for the benzene one by seven degrees, while for the fluorine substituted complexes the X···O−C is six degrees smaller for the halogen bonding complex compared to the hydrogen bonding one. These results may be a result of intermolecular interactions, likely to be more important when the molecules are closer together, as they are in the hydrogen bonding cases.

SAPT Results. Table 4 gives interaction energy decompositions in terms of symmetry-adapted perturbation theory (SAPT/aug-cc-pVDZ) for the complexes of bromobenzene and **4** with acetone. The most important aspect of these data is the fact that the interaction of **4** is much more electrostatic in nature than that of bromobenzene (by about a factor of 4). This result is not unexpected because the bromine $V_{S,max}$ for **4** is so much larger than that of bromobenzene (see Tables 1 and 2 and Figures 1B and 2C). The other three SAPT terms are also larger for **4** than for bromobenzene. The increase in induction is most likely caused by a larger degree of charge transfer for the **4**···acetone complex. The increases in both the dispersion and exchange terms can be attributed to the fact that in the **4**···acetone complex, the bromine is in much closer to the acetone oxygen than in the bromobenzene complex.

These results are in agreement with those in earlier work by Riley and Hobza.[11] There it was found that in the

interaction of unsubstituted bromomethane with formaldehyde, the SAPT electrostatic term contributes about 26% less than the dispersion term. Upon substitution of three fluorines to bromomethane to form F_3CBr, the size and positive potential of the bromine σ-hole increases significantly. Likewise, the electrostatic component of the interaction increases considerably, contributing about 37% *more* than dispersion.

Conclusions

The main conclusion to be drawn from this investigation is that the strength and character of halogen-bonding interactions can be influenced to a great extent through the introduction of various substituents onto an aromatic ring bearing bromine (or presumably other halogens such as chlorine and iodine). The range of interaction energies for the substituent configurations used in this study is quite large, varying from −1.80 kcal/mol (3,5-diaminobromobenzene) to −7.11 kcal/mol ($C_4N_2O_2HBr$, **4**). This result has great implications in the fields of drug design and crystal engineering, in which halogen bonding interactions have been the subject of intense research because of their unique properties and their potential in the development of novel pharmaceuticals and materials.

The principal mechanism for the modulation of halogen bond strengths by aromatic substitution involves changes in the electron density on bromine. It can be seen by studying the electrostatic potentials of these molecules that the presence of electron-withdrawing and -donating substituents greatly affects the electrostatic potential in the space around bromine (and the rest of the system). The introduction of different substituents into these systems produces a broad spectrum of bromine $V_{S,max}$ values (which measure the maximum positive potential found on the bromine surface), ranging from 4.9 kcal/mol (3,5-diaminobromobenzene) to 45.6 kcal/mol ($C_4N_2O_2HBr$, **4**). These $V_{S,max}$ values correlate very well with interaction energies, showing that the electrostatic properties of a possible halogen-bonding molecule are critical to its binding behavior. These findings are supported by SAPT interaction energy decompositions, which demonstrate that the electrostatic component of halogen bonding changes substantially upon substitution of a strong electron-withdrawing group or ring atom.

In cases where an electron-donating substituent (NH_2), no substituent (H), and weakly electron-withdrawing substituents (OH, Cl) are present, the bromine exhibits a conventional σ-hole, which varies greatly in size and in positive potential ($V_{S,max}$) and for which the bromines have rings of negative potentials around their lateral sides. For stronger electron-withdrawing substituents (=O, CN), the entire bromine acquires a positive potential, with a higher $V_{S,max}$, which leads to very stable halogen-bonding interactions. As would be expected, electron-donating groups tend to weaken halogen bonding, while electron-withdrawing substituents lead to stronger interactions. It should also be noted that for (unsubstituted and substituted) bromopyrimidines, which contain two electron-attracting nitrogens within their aromatic rings, the σ-hole is generally larger and more positive than for the corresponding bromobenzene structures.

Br···O Complexes as Probes

J. Chem. Theory Comput., Vol. 5, No. 1, 2009 **163**

As was expected, the optimum C−Br···O angles for halogen bonding complexes was found to be 180° (Figure 7), corresponding to an optimal interaction between the acetone oxygen and the bromine σ-hole. The strengths of these interactions decrease rather sharply as the C−Br···O angle becomes smaller and the σ-hole can no longer interact with =O. The C=O···Br angles for these complexes were observed to be in the range between 119° and 129°, with a tendency for stronger halogen-bonding interactions to assume larger angles. This trend is most likely attributable to the fact that stronger halogen bonds, with σ-holes that are more positive, will have a stronger tendency to line up with the most negative region of the acetone oxygen (found at a C=O···Br angle of ∼127°).

References

(1) Auffinger, P.; Hays, F. A.; Westhof, E.; Ho, P. S. *Proc. Natl. Acad. Sci. U.S.A.* **2004**, *101*, 16789–16794.

(2) Metrangolo, P.; Neukirsch, H.; Pilati, T.; Resnati, G. *Acc. Chem. Res.* **2005**, *38*, 386–395.

(3) Halogen Bonding with Dihalogens and Interhalogens, in Halogen Bonding. In *Fundamentals and Applications*; Metrangolo, P., Resnati, G., Eds.; Structure and Bonding 126; Springer: Berlin, 2008.

(4) Politzer, P.; Lane, P.; Concha, M. C.; Ma, Y.; Murray, J. S. *J. Mol. Model.* **2007**, *13*, 305–311.

(5) Brinck, T.; Murray, J. S.; Politzer, P. *Int. J. Quantum Chem., Quantum Biol. Symp.* **1992**, *19*, 57–64.

(6) Politzer, P.; Murray, J. S.; Concha, M. C. *J. Mol. Model.* **2007**, *13*, 643–650.

(7) Clark, T.; Hennemann, M.; Murray, J. S.; Politzer, P. *J. Mol. Model.* **2007**, *13*, 291–296.

(8) Murray, J. S.; Lane, P.; Politzer, P *Int. J. Quantum Chem.* **2007**, *107*, 3046–3052.

(9) Murray, J. S.; Lane, P.; Clark, T.; Politzer, P. *J. Mol. Model.* **2007**, *13*, 1033–1038.

(10) Politzer, P.; Murray, J. S.; Lane, P *Int. J. Quantum Chem.* **2007**, *107*, 3046–3052s.

(11) Riley, K. E.; Hobza, P. *J. Chem. Theory Comput.* **2008**, *4*, 232–242.

(12) Riley, K. E.; Merz, K. M. *J. Phys. Chem. A* **2007**, *111*, 1688–1694.

(13) Lommerse, J. P. M.; Stone, A. J.; Taylor, R.; Allen, F. H. *J. Am. Chem. Soc.* **1996**, *118*, 3108–3116.

(14) Lu, Y. X.; Zou, J. W.; Wang, Y. H.; Yu, Q. S. *J. Mol. Struct. Theochem* **2006**, *767*, 139–142.

(15) Poleshchuk, O. K.; Branchadell, V.; Brycki, B.; Fateev, A. V.; Legon, A. C. *J. Mol. Struct. Theochem* **2006**, *760*, 175–182.

(16) Palusiak, M.; Grabowski, S. *J. Struct. Chem.* **2008**, *19*, 5–11.

(17) Chopra, D; Thiruvenkatam, V.; Manjunath, S. G.; Row, T. N. G. *Cryst. Growth Des.* **2007**, *7*, 868–874.

(18) Corradi, E.; Meille, S. V.; Messina, M. T.; Metrangolo, P.; Resnati, G. *Ang. Chem., Int. Ed.* **2000**, *39*, 1782–1786.

(19) Glaser, R.; Chen, N. J.; Wu, H.; Knotts, N.; Kaupp, M. *J. Am. Chem. Soc.* **2004**, *126*, 4412–4419.

(20) Metrangolo, P.; Resnati, G. *Science* **2008**, *321*, 918–919.

(21) *Halogen Bonding: Fundamentals and Applications*; Metrangolo, P., Resnati, G. Eds.; Structure and Bonding 126; Springer: Berlin, 2008.

(22) Boys, S. F.; Bernardi, F. *Mol. Phys.* **1970**, *19*, 553–566.

(23) Stewart, R. F. *Chem. Phys. Lett.* **1979**, *65*, 335–342.

(24) *Chemical Applications of Atomic and Molecular Electrostatic Potentials*; Politzer, P., Truhlar, D. G., Eds.; Plenum, New York, 1981.

(25) Bader, R. F. W.; Carroll, M. T.; Cheeseman, J. R.; Chang, C. *J. Am. Chem. Soc.* **1987**, *109*, 7968–7979.

(26) Murray, J. S.; Politzer, P. *J. Mol. Struct. (Theochem)* **1998**, *425*, 107–114.

(27) Politzer, P.; Murray, J. S. *Fluid Phase Equilib.* **2001**, *185*, 129–137.

(28) Hagelin, H.; Murray, J. S.; Brinck, T.; Berthelot, M.; Politzer, P *Can. J. Chem.* **1995**, *73*, 483–488.

(29) Jeziorski, B.; Moszynski, R.; Szalewicz, K. *Chem. Rev.* **1994**, *94*, 1887–1930.

(30) Werner, H. J.; Knowles, P. J.; Lindh, R.; Manby, F. R.; Schütz, M.; Celani, P.; Korona, T.; Rauhut, G.; Amos, R. D.; Bernhardsson, A.; Berning, A.; Cooper, D. L.; Deegan, M. J. O.; Dobbyn, A. J.; Eckert, F.; Hampel, C.; Hetzer, G.; Lloyd, A. W.; McNicholas, S. J.; Meyer, W.; Mura, M. E.; Nicklaβ; A.; Palmieri, P.; Pitzer, R.; Schumann, U.; Stoll, H.; Stone, A. J.; Tarroni, R.; T., T. *Molpro*, version 2006.1; 2006.

(31) Bondi, A. *J. Phys. Chem.* **1964**, *68*, 441–451.

(32) Clark, T.; Murray, J. S.; Lane, P.; Politzer, P. *J. Mol. Model.* **2008**, *14*, 689–697.